

Microwave Measurement of Dielectric Properties of Low-Loss Materials by the Dielectric Rod Resonator Method

YOSHIO KOBAYASHI, MEMBER, IEEE, AND MASAYUKI KATOH

Abstract — Improvements both in accuracy and speed are described for the technique of measuring the microwave dielectric properties of low-loss materials by using a dielectric rod resonator short-circuited at both ends by two parallel conducting plates. A technique for measuring the effective surface resistance R_s of the conducting plates is proposed to allow the accurate measurement of the loss tangent $\tan \delta$. By means of the first-order approximation, the expressions are analytically derived for estimating the errors of the measured values of relative permittivity ϵ_r , $\tan \delta$, and R_s , for measuring the temperature coefficient of ϵ_r , and for determining the required size of the conducting plates. Computer-aided measurements are realized by using these expressions. It is shown that the temperature dependence of R_s should be considered in the $\tan \delta$ measurement. The copper plates used in this experiment have the relative conductivity of 91.0 ± 2.7 percent at 20°C , estimated from the measured R_s value. For a 99.9-percent alumina ceramic rod sample, the results measured at 7.69 GHz and 25°C show that $\epsilon_r = 9.687 \pm 0.003$ and $\tan \delta = (1.6 \pm 0.2) \times 10^{-5}$. The temperature coefficients measured between 25 and 100°C are $112 \times 10^{-6}/^\circ\text{C}$ for ϵ_r and $23 \times 10^{-4}/^\circ\text{C}$ for $\tan \delta$.

I. INTRODUCTION

A DIELECTRIC ROD resonator short-circuited at both ends by two parallel conducting plates is widely used to measure the dielectric properties of high-permittivity and low-loss materials in the microwave region [1]–[6]. For the measurement of the relative permittivity ϵ_r , a high accuracy within 0.1 percent can be obtained easily from this method. For the measurement of the loss tangent $\tan \delta$, however, its accuracy is considerably restricted by the uncertainty in the actual value of the surface resistance R_s of the conducting plates, as discussed by Courtney [3]. It becomes particularly severe for $\tan \delta < 5 \times 10^{-4}$. As compared with that calculated using dc bulk conductivity, the R_s value is effectively increased not only by surface roughness, oxidation, scratches, etc. [7], [8], but also by the excess conductor loss due to the coupling elements attached. We should also take account of the temperature dependence of R_s .

In this paper, a technique for measuring the effective value of R_s involving all effects described above is proposed to allow the accurate measurement of $\tan \delta$. To put this technique into practice, the precise design of two

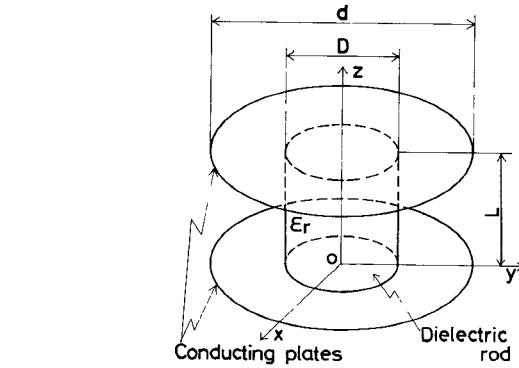


Fig. 1. Configuration of a dielectric rod resonator short circuited at both ends by two parallel conducting plates.

dielectric rod resonators with different lengths and a clear identification of the TE_{011} and TE_{01l} ($l \geq 2$) resonant modes from other modes are required. They can be realized successfully by the use of mode charts presented in a previous paper [9]. Furthermore, the expressions for estimating the errors of the measured values of ϵ_r , $\tan \delta$, and R_s , for measuring the temperature coefficient of ϵ_r , and for determining the required size of the conducting plates, are derived analytically by means of the first-order approximation. Computer-aided measurements are realized by using these expressions. The availability of this method is verified by actual dielectric measurements.

II. GENERAL ANALYSIS

A. Measurement of Complex Permittivity

A configuration of a dielectric rod resonator used in the dielectric measurement is shown in Fig. 1. Here a cylindrical dielectric rod sample of diameter D and length L is placed between two parallel conducting plates of diameter d . The required size of d will be discussed later. The permeability of the rod is assumed to be equal to that of a vacuum. The values of ϵ_r and $\tan \delta$ of the rod can be obtained from the measured values of the resonant frequency f_0 and the unloaded Q , Q_u for the TE_{0ml} mode this resonator.

At first, ϵ_r is given by [1], [2]

$$\epsilon_r = \left(\frac{\lambda_0}{\pi D} \right)^2 (u^2 + v^2) + 1 \quad (1)$$

Manuscript received October 2, 1984; revised February 11, 1985.

The authors are with the Department of Electrical Engineering, Saitama University, Urawa, Saitama, 338 Japan.

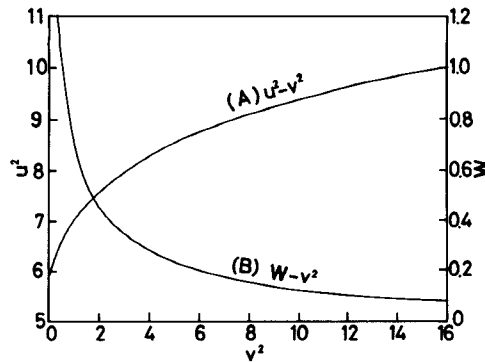


Fig. 2. Chart for complex permittivity measurements (TE_{01l} mode).

where

$$v^2 = \left(\frac{\pi D}{\lambda_0} \right)^2 \left[\left(\frac{\lambda_0}{\lambda_g} \right)^2 - 1 \right] \quad (2)$$

$$\lambda_0 = \frac{c}{f_0}, \quad \lambda_g = \frac{2L}{l}, \quad l = 1, 2, \dots \quad (3)$$

Here, λ_0 is the resonant wavelength, c is the light velocity in a vacuum, and λ_g corresponds to the guiding wavelength of an infinitely long dielectric rod waveguide. Furthermore, u^2 is related to v^2 by the following transcendental equation:

$$u \frac{J_0(u)}{J_1(u)} = -v \frac{K_0(v)}{K_1(v)} \quad (4)$$

where $J_n(u)$ is the Bessel function of the first kind and $K_n(v)$ is the modified Bessel function of the second kind. For any value of v , the m th solution u exists between u_{0m} and u_{1m} , where $J_0(u_{0m}) = 0$ and $J_1(u_{1m}) = 0$. The first solution ($m = 1$) is shown in Fig. 2 by curve A.

In the following, $\tan \delta$ is given by Hakki and Coleman [1] as

$$\tan \delta = \frac{A}{Q_u} - BR_s \quad (5)$$

where

$$A = 1 + \frac{W}{\epsilon_r} \quad (6)$$

$$B = \left(\frac{\lambda_0}{\lambda_g} \right)^3 \frac{1 + W}{30\pi^2 \epsilon_r l} \quad (7)$$

$$W = \frac{J_1^2(u)}{K_1^2(v)} \frac{K_0(v)K_2(v) - K_1^2(v)}{J_1^2(u) - J_0(u)J_2(u)} \quad (8)$$

$$R_s = \sqrt{\frac{\pi f_0 \mu}{\sigma}} = 0.825 \times 10^{-2} \sqrt{\frac{f_0 [\text{GHz}]}{\bar{\sigma}}} [\Omega], \quad \bar{\sigma} = \frac{\sigma}{\sigma_0}. \quad (9)$$

The function W , which is the ratio of electric-field energy stored outside to inside the rod [10], is represented as the function of v , for u is the function of v in (4). The computed result of (8) for $m = 1$ is shown in Fig. 2 by curve B. As v increases, W decreases monotonically; more

energy is concentrated into the rod. Also, the conductivity σ and the relative conductivity $\bar{\sigma}$ are the effective values associated with R_s . The second expression of (9) was calculated using the conductivity of the international standard annealed copper, $\sigma_0 = 5.8 \times 10^7 \text{ S/m}$, and the permeability for a nonmagnetic metal, $\mu = \mu_0 = 4\pi \times 10^{-7} \text{ H/m}$.

B. Measurement of Surface Resistance

For low-loss materials having $\tan \delta$ below 5×10^{-4} , the terms A/Q_u and BR_s in (5) are of the same orders of magnitude when the TE₀₁₁ mode is used. Therefore, the accurate effective value of R_s at the temperature in the measurement is required to measure $\tan \delta$ with high accuracy; so a technique to measure R_s using the same instrument as used for the dielectric measurement, as in Fig. 1, was developed. In this technique, we use two rod samples cut from a dielectric rod, which have the same diameters but different lengths; one rod for a TE_{01l} resonator is l times as long as the other for a TE₀₁₁ resonator, where $l \geq 2$. We denote the quantities for both resonators by subscripts l and 1, respectively. While $f_{0l} = f_{01}$, it follows that $Q_{ul} > Q_{u1}$ because of the different effects of conductor loss on the Q_u values. Owing to the fact that both rods have the same $\tan \delta$ values, (5) yields

$$R_s = 30\pi^2 \left(\frac{\lambda_g}{\lambda_0} \right)^3 \frac{\epsilon_r + W}{1 + W} \frac{l}{l-1} \left(\frac{1}{Q_{u1}} - \frac{1}{Q_{ul}} \right). \quad (10)$$

Thus, R_s and $\bar{\sigma}$ in (9), can be determined from the measured values of Q_{u1} and Q_{ul} . The difference between the Q_{ul} and Q_{u1} values increases with ϵ_r and l ; more precise R_s measurement can be attained as seen in (22) derived later. The substitution of (10) into (5) yields

$$\tan \delta = \frac{A}{l-1} \left(\frac{l}{Q_{ul}} - \frac{1}{Q_{u1}} \right) \quad (11)$$

which is independent of R_s and therefore allows precise measurement of $\tan \delta$. It is difficult to precisely machine samples to the designed dimensions. In this case, we use the following expressions instead of (10) and (11):

$$R_s(f_0) = \frac{1}{C_1 - C_l} \left(\frac{A_1}{Q_{u1}} - \frac{A_l}{Q_{ul}} \right) \quad (12)$$

$$\tan \delta = \frac{C_1}{C_1 - C_l} \left(\frac{A_l}{Q_{ul}} - \frac{C_l}{C_1} \frac{A_1}{Q_{u1}} \right) \quad (13)$$

which are derived from (5) by using the relations

$$R_{sl}(f_{0l}) = \sqrt{\frac{f_{0l}}{f_0}} R_s(f_0), \quad C_l = B_l \sqrt{\frac{f_{0l}}{f_0}} \quad (14)$$

where f_0 is chosen arbitrarily near f_{01} and f_{0l} .

C. Preparation of Rod Sample

In the design of the resonators, at first, the trapped state condition for the TE_{0ml} mode must be satisfied [9]; that is,

$$\frac{D}{L} > x_c, \quad x_c = \frac{2u_{0m}}{l\pi\sqrt{\epsilon_r - 1}}, \quad J_0(u_{0m}) = 0 \quad (15)$$

where x_c is a cutoff value of the TE_{0ml} mode. In this state, the energy is trapped in and near the rod, while for $D/L < x_c$, the resonance is in the leaky state, which is not suitable for the measurement since the energy leaks out in the radial direction. As ϵ_r to be measured is lower, a larger value of D/L is needed. Additionally, the proper rod dimensions must be determined with good mode separation lest the TE_{0ml} mode be disturbed by the adjacent modes. The mode charts are useful for this purpose [9]. For the TE_{011} mode with $\epsilon_r \geq 10$, for example, the range of $D/L = 1.4$ to 1.8 should be avoided because there are the low- Q leaky state modes TM_{210} and TM_{020} near this mode. In this case, the suitable ranges are $D/L = 1.0$ –1.3, 1.9–2.3, 3.0–3.3, etc.

D. Error Estimation of Measured Values

The expressions for estimating the mean-square errors of the measured values ϵ_r , $\tan \delta$, and R_s were derived by means of the first-order approximation. Let the small change of any quantity x be Δx . The error of ϵ_r in (1) is mainly determined by the errors of D , L , and f_0 . Then $\Delta \epsilon_r$ is given by (see Appendix)

$$\Delta \epsilon_r = \Delta \epsilon D + \Delta \epsilon L + \Delta \epsilon f \quad (16)$$

where

$$\Delta \epsilon D = -2(\epsilon_r - 1) \frac{u^2 - v^2 W}{u^2 + v^2} \frac{\Delta D}{D} \quad (17)$$

$$\Delta \epsilon L = -2(1 + W) \frac{u^2 + \epsilon_r v^2}{u^2 + v^2} \frac{\Delta L}{L} \quad (18)$$

$$\Delta \epsilon f = -2(\epsilon_r + W) \frac{\Delta f_0}{f_0}. \quad (19)$$

When the mean-square errors $\overline{\Delta D}$, $\overline{\Delta L}$, and $\overline{\Delta f_0}$ are estimated, the mean-square error $\overline{\Delta \epsilon_r}$ can be estimated from

$$(\overline{\Delta \epsilon_r})^2 = (\overline{\Delta \epsilon D})^2 + (\overline{\Delta \epsilon L})^2 + (\overline{\Delta \epsilon f})^2. \quad (20)$$

A similar procedure is followed for the error estimation of the other quantities. The error of $\tan \delta$ in (5) determined mainly by the errors of Q_u and R_s (or σ) is estimated from

$$\Delta \tan \delta = -\frac{A}{Q_u} \frac{\Delta Q_u}{Q_u} - BR_s \frac{\Delta R_s}{R_s} = -\frac{A}{Q_u} \frac{\Delta Q_u}{Q_u} + \frac{BR_s}{2} \frac{\Delta \sigma}{\sigma}. \quad (21)$$

Also, the errors of R_s and $\tan \delta$ in (10) to (13) determined mainly by the errors of Q_{ul} and Q_{ul} are estimated, respectively, from

$$\Delta R_s = \frac{R_s}{Q_{ul} - Q_{ul}} \left(Q_{ul} \frac{\Delta Q_{ul}}{Q_{ul}} - Q_{ul} \frac{\Delta Q_{ul}}{Q_{ul}} \right) \quad (22)$$

$$\Delta \tan \delta = \frac{\tan \delta}{lQ_{ul} - Q_{ul}} \left(lQ_{ul} \frac{\Delta Q_{ul}}{Q_{ul}} - Q_{ul} \frac{\Delta Q_{ul}}{Q_{ul}} \right). \quad (23)$$

The effects of the other error factors $\Delta \epsilon_r$, ΔD , ΔL , Δf_0 , etc., on ΔR_s and $\Delta \tan \delta$ are very small.

E. Measurement of Temperature Dependence of Complex Permittivity

We first consider the case of ϵ_r . If the small linear changes $\Delta \epsilon_r$, ΔD , ΔL , and Δf_0 in (16)–(19) are caused by

the temperature change $\Delta T^\circ C$ of the structure, the following simple expression is derived from dividing both sides of (16) by $\epsilon_r \Delta T$:

$$\tau_\epsilon = -2 \left(1 + \frac{W}{\epsilon_r} \right) (\tau_f + \tau_L) \quad (24)$$

where

$$\tau_\epsilon = \frac{1}{\epsilon_r} \frac{\Delta \epsilon_r}{\Delta T}, \quad \tau_f = \frac{1}{f_0} \frac{\Delta f_0}{\Delta T}, \quad \tau_L = \frac{1}{L} \frac{\Delta L}{\Delta T} = \frac{1}{D} \frac{\Delta D}{\Delta T}. \quad (25)$$

Here, τ_ϵ is the temperature coefficient of ϵ_r , τ_f is the temperature coefficient of f_0 , and τ_L is the coefficient of the thermal linear expansion of the rod assumed to be isotropic. Thus, τ_ϵ can be obtained from the measured values of τ_f and τ_L .

When the temperature dependence of $\tan \delta$ is measured, that of R_s or σ should be taken into account. At DC , the relation between $\sigma(T)$ at temperature $T^\circ C$ and $\sigma(T_0)$ at temperature $T_0^\circ C$ is given, in customary form, by

$$\sigma(T) = \frac{\sigma(T_0)}{1 + \alpha(T - T_0)} \quad (26)$$

where α is the temperature coefficient of the resistivity $1/\sigma$, e.g., the published value for copper is $\alpha = 3.93 \times 10^{-3}$ at $T_0 = 20^\circ C$. Assuming the relation is held in the microwave region as well, we can rewrite (5) as follows:

$$\tan \delta(T) = \frac{A}{Q_u(T)} - BR_{s0} \sqrt{1 + \alpha(T - T_0)} \quad (27)$$

with $R_{s0} = (\pi f_0 \mu / \sigma(T_0))^{1/2}$. Here, we may assume that A , B , and R_{s0} remain constant on the temperature change, since the changes of D , L , f_0 , and ϵ_r are usually small. Also, the relation between $\Delta Q_u(T)$ and $\Delta \tan \delta(T)$, both caused by the change from T_0 to T , is derived from (27) by means of the first-order approximation and is given by

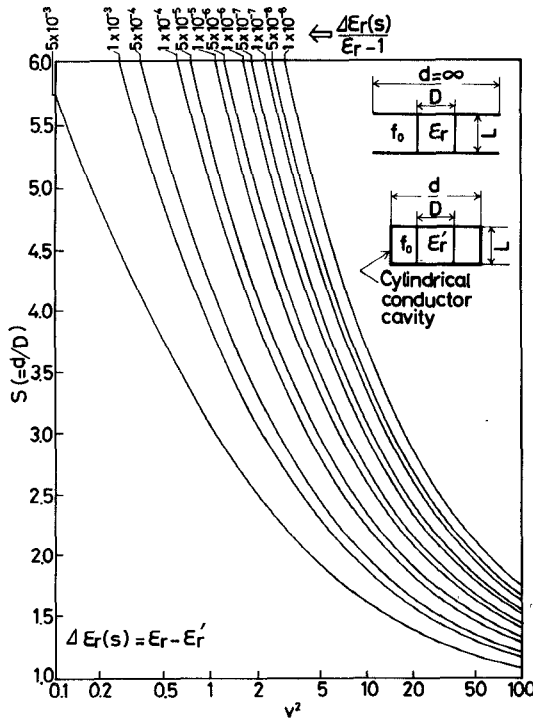
$$\Delta \tan \delta(T) = \frac{A}{Q_u} \frac{\Delta Q_u(T)}{Q_u} - \frac{1}{2} \alpha BR_{s0} (T - T_0). \quad (28)$$

If putting $\Delta \tan \delta(T) = 0$ in (28), we can calculate $\Delta Q_u(T)/Q_u$ caused by α alone; e.g., for the cases $\epsilon_r = 37.7$ and 9.8, treated later, we obtain $\Delta Q_u(T)/Q_u = 0.120$ and 0.167 for copper when $T - T_0 = 100^\circ C$, respectively. These magnitudes could never be neglected since the precision in the Q_u measurement is about 1 percent.

F. Required Size of Conducting Plates

In the analysis described above, the conducting plates have been assumed to be infinitely large ($d = \infty$). In practice, however, since the field outside the rod decays rapidly in the radial direction, a suitable finite size of the plates is permitted, in so far as the influence on the measurement is negligibly small.

Let ϵ_r and $\tan \delta$ be the values obtained from given values of f_0 and Q_u for a structure in the case of $d = \infty$. Then define $\Delta \epsilon_r(S)$ by $\Delta \epsilon_r(S) = \epsilon_r - \epsilon'_r$, where ϵ'_r is obtained from the same f_0 value for a structure short-circuited with a conducting ring of diameter d , as illustrated in Fig. 3. Also define $\Delta \tan \delta(S)$ by $\Delta \tan \delta(S) = \tan \delta -$

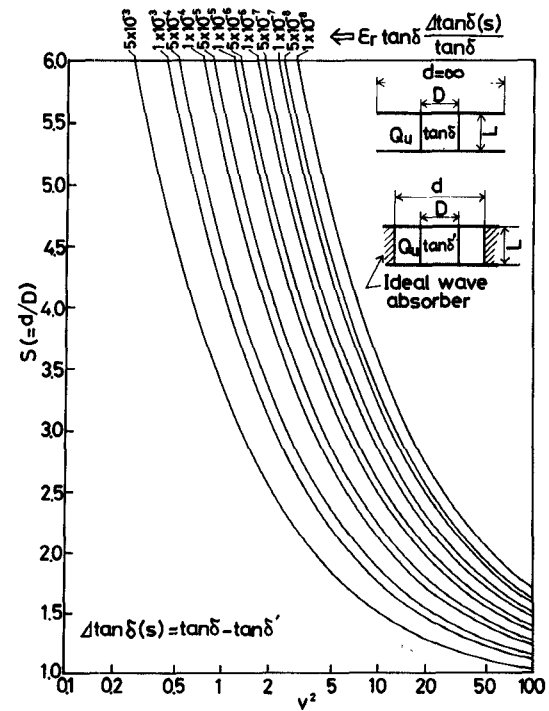
Fig. 3. Size ratio S required for the permissible error $\Delta\epsilon_r(S)$.

$\tan\delta'$, where $\tan\delta'$ is obtained from the same Q_u value for a structure enclosed with an ideal wave absorber, in which the energy is perfectly dissipated without reflection, as illustrated in Fig. 4. If $d = \infty$, $\Delta\epsilon_r(S) = 0$ and $\Delta\tan\delta(S) = 0$. The required size ratio $S = d/D$ can be determined analytically from the viewpoint of the permissible magnitudes of $\Delta\epsilon_r(S)$ and $\Delta\tan\delta(S)$. They are expressed by

$$\frac{\Delta\epsilon_r(S)}{\epsilon_r - 1} = \frac{g(v)}{f'(u)} \frac{2u}{u^2 + v^2} \left[\frac{I_0(v)}{K_0(v)} + \frac{I_1(v)}{K_1(v)} \right] \frac{K_1(Sv)}{I_1(Sv)} \quad (29)$$

$$\epsilon_r \Delta\tan\delta(S) = SW \frac{K_0(Sv)K_2(Sv) - K_1^2(Sv)}{K_0(v)K_2(v) - K_1^2(v)} \quad (30)$$

where the functions $g(v)$ and $f'(u)$ are given by (34) and (35) in the Appendix, and $I_n(v)$ is the modified Bessel function of the first kind. The derivations are described elsewhere [10]. The results computed from (29) and (30) are shown in Figs. 3 and 4, respectively. As v is smaller, the energy stored outside the rod increases and then the larger value of S is needed. Since $\Delta\epsilon_r/\epsilon_r$ of 0.1 percent is attained easily, the S value should be sufficiently large to satisfy $\Delta\epsilon_r(S)/\epsilon_r < 0.01$ percent at least. For low-loss materials, the influence of S on $\tan\delta$ is more severe than that on ϵ_r . For example, if a sample having $\epsilon_r = 10$ and $\tan\delta = 10^{-4}$ is measured at $v^2 = 2.6$ and $S = 3.5$ at which two curves for $\Delta\epsilon_r(S)/(\epsilon_r - 1) = 10^{-4}$ in Fig. 3 and $\epsilon_r \Delta\tan\delta(S) = 10^{-4}$ in Fig. 4 intersect, then $\Delta\epsilon_r(S)/\epsilon_r$ is attained of 0.01 percent, but $\Delta\tan\delta(S)/\tan\delta$ becomes 10 percent, which is too large.

Fig. 4. Size ratio S required for the permissible error $\Delta\tan\delta(S)$.

G. Computer-Aided Measurements

Graphical calculations described above are rather tedious and there are many opportunities for errors. Then a BASIC program for a personal computer (NEC: PC-9801) was developed. In the calculation of ϵ_r , the Newton-Raphson iterative procedure was used to solve (4). The right side of (4) is first calculated after the v value is determined from the measured values. As an initial value of u , u_{0m} is then tried in (4) and then sufficient iterations are performed to give a solution. Once the solution u is obtained, other quantities can be easily calculated from the expressions derived above. Thus, outputs ϵ_r , $\tan\delta$, $\Delta\epsilon_r$, $\Delta\tan\delta$, $\Delta\epsilon_r(S)$, and $\Delta\tan\delta(S)$ were obtained from inputs m , l (for TE_{0ml}), D , L , f_0 , Q_u , T , $\bar{\sigma}(20^\circ\text{C})$, \bar{D} , \bar{L} , \bar{f}_0 , \bar{Q}_u , $\bar{\sigma}$, and d . It takes only 30 seconds for a single run.

III. EXPERIMENT

A. Dielectrometer

A photograph of a dielectrometer used in the measurement is shown in Fig. 5. It is simply constructed from a disk-type micrometer with parallel measuring faces 20 mm in diameter, two flat conducting plates, and two semi-rigid coaxial cables, each of which has a small loop at the top. As instant adhesives, a minimum amount of grease was used to hold the conducting plates on the upper and lower measuring faces of the micrometer. A dielectric rod sample is placed near the center on the lower plate. Then the upper plate is lowered to gently touch the top face of the rod so that the rod length is not changed by excessive mechanical pressure. A transmission-type resonator was constructed and undercoupled equally to the input and output loops. The resonant frequency f_0 for the TE_{0ml} mode, the

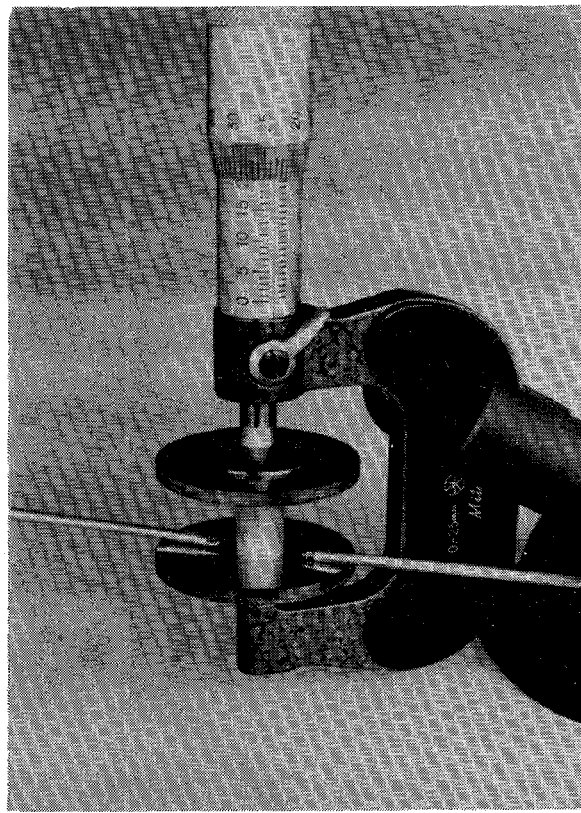


Fig. 5. Photograph of a dielectrometer used in the measurement.

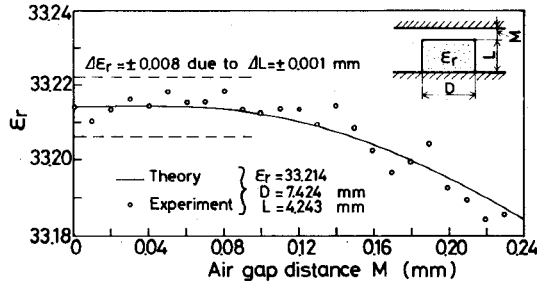


Fig. 6. Air-gap effect on the permittivity measurement.

half-power band width $f_2 - f_1$, and the insertion loss IL_0 [dB] at f_0 were measured using an HP Network Analyzer 8410S by means of the swept-frequency method. In the experiment, the shift of f_0 due to field disturbances was to within 0.001 percent when $IL_0 > 20$ dB. Also, the unloaded Q , Q_u is obtained from the loaded Q , Q_L as follows [11]:

$$Q_u = \frac{Q_L}{1 - a_t}, \quad Q_L = \frac{f_0}{f_2 - f_1}, \quad a_t = 10^{-IL_0[\text{dB}]/20}. \quad (31)$$

B. Discussion of Air-Gap Effect

We use the mean diameter \bar{D} as D , and the maximum length L_m (i.e., the distance between two conducting plates) as L . In this case, it is asserted [2] that air-gaps at the rod-plate interfaces do not affect the measurement. This verification is given in Fig. 6. In the figure, the open dots show the experimental $\bar{\epsilon}_r$ values obtained from (1) by

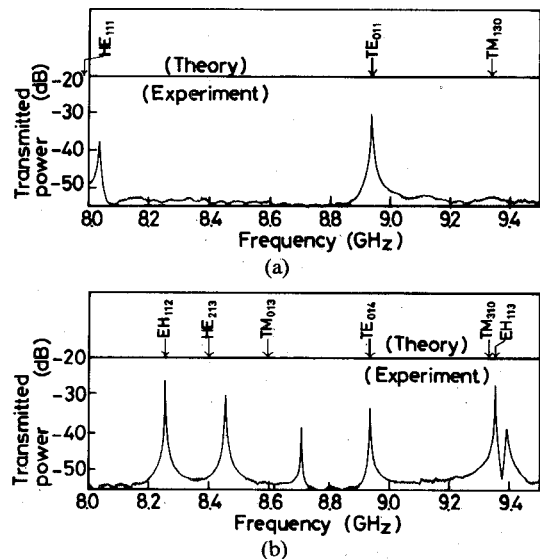


Fig. 7. Frequency responses for TE_{011} and TE_{014} resonators with $\epsilon_r = 37.6$ and $D = 8.50$ mm. (a) TE_{011} resonator ($L = 3.572$ mm). (b) TE_{014} resonator ($L = 14.276$ mm).

using the f_0 values measured as the air-gap distance M is varied and the assumed rod lengths $L + M$. In a similar way, a theoretical curve indicated by the solid line was obtained from the f_0 values versus M accurately computed for the TE_{018} mode by the mode-matching technique [12]. The agreement between both results is well within the scatter $\Delta\epsilon_r = \pm 0.008$, which corresponds to the uncertainty in sample length $\Delta L = \pm 0.001$ mm. For $M < 0.1$ mm, the air-gap effect is not observed, while for $M > 0.1$ mm, it apparently decreases the $\bar{\epsilon}_r$ values. Thus, the air-gap effect is negligible since it is feasible to finish the rod surface to within 0.01 mm.

C. Measured Results

Two samples for the R_s measurement were cut from a $(\text{Zr-Sn})\text{TiO}_4$ ceramic rod of $\epsilon_r = 37.6$, $\tan\delta = 1.8 \times 10^{-4}$, and $D = 8.5$ mm (Murata Mfg. Co., Ltd.): one is a disk of $D/L = 2.38$ for the TE_{011} resonator; the other is a rod of $D/L = 0.595$ for the TE_{014} resonator. These D/L values were determined from the mode charts [9]. The diameter d determined from Fig. 4 for $\Delta\tan\delta(S)/\tan\delta = 0.01$ percent is 23 mm. We used a pair of copper plates of $d = 70$ mm, and mechanically polished the inner surfaces which touch the rod.

In the experiment, the desired TE_{0ml} mode must be identified. The mode charts [9] are also useful for this purpose. The measured frequency responses for two resonators are shown in Fig. 7, together with the theoretical values. The measured resonant frequencies for the TE and EH modes agree well with the theoretical ones, while those for the TM and HE modes are increased by 1 to 5 percent because of the air-gap effect. The TE_{011} and TE_{014} modes were clearly identified. The measured results of ϵ_r , $\tan\delta$, R_s , and $\bar{\sigma}(20^\circ\text{C})$ are shown in Table I; their mean-square errors estimated are about 0.05, 1.1, 1.5, and 3.0 percent, respectively.

TABLE I
THE R_s AND $\bar{\sigma}$ VALUES OF COPPER PLATES MEASURED AT 23°C
AND THE MEAN-SQUARE ERRORS

Resonant Mode	TE ₀₁₁	TE ₀₁₄
D + \overline{D} [mm]	8.500 ± 0.002	8.503 ± 0.002
L _m + \overline{L}_m [mm]	3.572 ± 0.001	14.276 ± 0.001
f ₀ + \overline{f}_0 [mm]	8923.34 ± 1.42	8923.16 ± 0.35
Q _u + \overline{Q}_u [mm]	2237 ± 14	4040 ± 17
v ²	13.340	13.373
u ²	9.780	9.783
$\epsilon_r \pm \Delta \epsilon_r$	37.60 ± 0.02	37.63 ± 0.01
W	0.09846	0.09823
$\tan \delta \pm \Delta \tan \delta$	$(1.81 \pm 0.02) \times 10^{-4}$	
R _s (23°C) [Ω]	$(2.60 \pm 0.04) \times 10^{-2}$ at 8.92 GHz	
$\bar{\sigma}$ (23°C) [%]	90.0 ± 2.7	
$\bar{\sigma}$ (20°C) [%]	91.0 ± 2.7	

TABLE II
THE ϵ_r AND $\tan \delta$ VALUES OF 99.9-PERCENT ALUMINA
CERAMICS MEASURED AT 23°C AND THE MEAN-SQUARE ERRORS

Sample No.	No. 1	No. 2	No. 3
D ± \overline{D} [mm]	16.013 ± 0.001	16.006	16.006
L _m ± \overline{L}_m [mm]	9.239 ± 0.001	9.028	9.185
f ₀ ± \overline{f}_0 [MHz]	7688.51 ± 0.40	7780.4	7717.0
$\epsilon_r \pm \Delta \epsilon_r$	9.687 ± 0.002	9.706	9.680
Q _u ± \overline{Q}_u	9170 ± 90	8870	9170
$\sigma(20^\circ\text{C})$ [%]	91.0 ± 2.7	91.0	91.0
A/Q _u ($\times 10^{-5}$)	11.13 ± 0.11	11.51	11.14
BR _s ($\times 10^{-5}$)	9.54 ± 0.14	9.84	9.61
$\tan \delta$ ($\times 10^{-5}$)	1.59 ± 0.18	1.67	1.53

In the following, three samples of 99.9-percent alumina ceramics (NGR Spark Plug Co., Ltd.) were measured using these copper plates. The results of ϵ_r and $\tan \delta$ are shown in Table II; their mean-square errors are about 0.02 and 11.3 percent, respectively. This high precision for ϵ_r allows us to distinguish the scattering of the ϵ_r values for these samples. The errors $\Delta \epsilon_r(S) = 2.4 \times 10^{-7}$ and $\Delta \tan \delta(S) = 1.8 \times 10^{-9}$ estimated for $d = 70$ mm ($S = 4.73$) can be safely neglected. Even if the other errors are considered, sample No. 1 has $\epsilon_r = 9.687 \pm 0.03$ percent and $\tan \delta = 1.6 \times 10^{-5} \pm 12$ percent. In accuracy, these results compare favorably with the results for a single crystal sapphire rod, $\epsilon_r = 9.41 \pm 0.4$ percent and $\tan \delta = 1.5 \times 10^{-5} \pm 40$ percent, measured at the National Bureau of Standards and reported by Courtney [3].

To measure the temperature dependences of ϵ_r and $\tan \delta$ for sample No. 1, the resonator was placed in a temperature-stabilized oven as in Fig. 8; i.e., an upper copper plate was merely put on the top of a rod placed on a lower copper plate to secure free thermal expansion of the rod. The measured results for f_0 and Q_u are shown in Fig. 8. Then, the ϵ_r and $\tan \delta$ values versus temperature obtained from (1) and (27) by using these results and by considering the thermal expansion of rod dimensions are shown in Fig. 9. From Fig. 9, $\tau_\epsilon = 111.7$ ppm/°C is obtained, while $\tau_\epsilon = 111.4$ ppm/°C is estimated from (24) using $\tau_f = -59.94$ ppm/°C (Fig. 8) and $\tau_L = 5.4$ ppm/°C (between

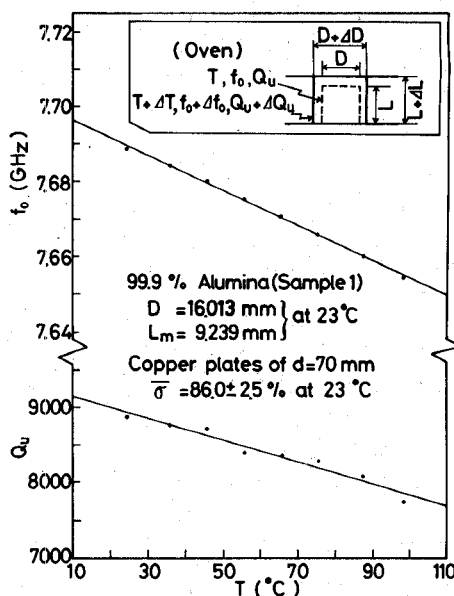


Fig. 8. Temperature dependence of f_0 and Q_u values measured for the TE₀₁₁ mode.

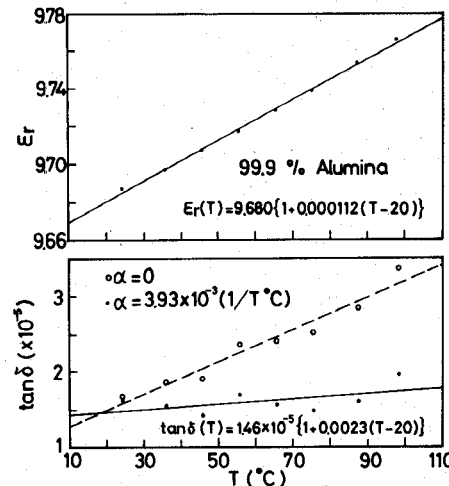


Fig. 9. Temperature dependence of ϵ_r and $\tan \delta$ values measured for 99.9-percent alumina ceramics (Sample No. 1).

20–100°C). Both τ_ϵ values are in good agreement; thus, the validity of (24) is verified. Furthermore, the comparison of two results for $\tan \delta$ in Fig. 9 with and without consideration of α shows the importance of taking the temperature dependence of R_s or σ into account.

D. Other Theoretical Errors of ϵ_r

The other errors included in the ϵ_r value obtained from (1) can be analytically derived by means of the first-order approximation. Thus, intrinsic permittivity ϵ_{ri} is given by

$$\epsilon_{ri} = \epsilon_r - 2 \left(\frac{\lambda_0}{\lambda_g} \right)^2 (1 + W) \frac{\delta_s}{L} - W(\epsilon_a - 1) - \frac{\epsilon_r + W}{4} (\tan \delta)^2 \quad (32)$$

with $\delta_s = 1/\sigma R_s$. The second term on the right side of (32) represents the correction for the skin depth δ_s of the conducting plates; the third term for the permittivity of

atmosphere surrounding the rod denoted ϵ_a ($\epsilon_a \approx 1.0008$ for the air); the fourth term for $\tan \delta$ of rod treated by Hakki and Coleman [1]. For example, the estimation from (32) for sample No. 1 alumina gives

$$\epsilon_{ri} = 9.687 - 0.92 \times 10^{-3} - 0.17 \times 10^{-3} - 0.63 \times 10^{-9} \\ \approx 9.687 - 0.001.$$

Thus, these errors can usually be neglected.

IV. CONCLUSION

The effective surface resistance of conducting plates R_s was determined accurately by measurement so that the accurate measurement of $\tan \delta$ was realized. The expressions useful for estimating the errors of the measured values ϵ_r , $\tan \delta$, and R_s , for measuring the temperature coefficient of ϵ_r , and for determining the required size of the conducting plates were derived by means of the first-order approximation so that the computer-aided measurement was realized. As a result, the dielectric rod resonator method was improved both in accuracy and speed.

The accuracy of this measurement is summarized as follows: it is within 0.1 percent for ϵ_r , about 1.5 percent for R_s , about 3 percent for σ , about 1.2 percent for $\tan \delta = 10^{-4}$, and about 12 percent for $\tan \delta = 10^{-5}$. Also, the resolution for the $\tan \delta$ measurement is the order of 10^{-6} .

APPENDIX

We rewrite (4) as follows:

$$f(u) = g(v) \quad (33)$$

where

$$f(u) = u \frac{J_0(u)}{J_1(u)}, \quad g(v) = -v \frac{K_0(v)}{K_1(v)}. \quad (34)$$

Then the differentiations of $f(u)$ and $g(v)$ are given by

$$\frac{df(u)}{du} = -u \frac{J_1^2(u) - J_0(u)J_2(u)}{J_1^2(u)} = f'(u) \quad (35)$$

$$\frac{dg(v)}{dv} = -v \frac{K_0(v)K_2(v) - K_1^2(v)}{K_1^2(v)}. \quad (36)$$

From (33), (35), and (36), we obtain the relation

$$\frac{du^2}{dv^2} = \frac{udu}{vdv} = \frac{u}{v} \frac{du}{df(u)} \frac{dg(v)}{dv} = W \quad (37)$$

where W is given by (8). Then the propagation of error of (1) is expressed by

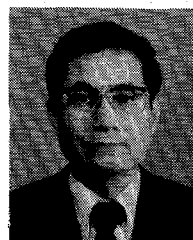
$$\Delta \epsilon_r = \frac{\partial \epsilon_r}{\partial D} \Delta D + \frac{\partial \epsilon_r}{\partial L} \Delta L + \frac{\partial \epsilon_r}{\partial f_0} \Delta f_0. \quad (38)$$

Then, we obtain (16) through (19) from calculating each term of (38) using (37).

REFERENCES

- [1] B. W. Hakki and P. D. Coleman, "A dielectric resonator method of measuring inductive capacities in the millimeter range," *IRE Trans. Microwave Theory Tech.*, vol. MTT-8, pp. 402-410, July 1960.
- [2] S. B. Cohn and K. C. Kelly, "Microwave measurement of high-dielectric constant materials," *IEEE Trans. Microwave Theory Tech.*, vol. MTT-14, pp. 406-410, Sept. 1966.
- [3] W. E. Courtney, "Analysis and evaluation of a method of measuring the complex permittivity and permeability of microwave insulators," *IEEE Trans. Microwave Theory Tech.*, vol. MTT-18, pp. 476-485, Aug. 1970.
- [4] W. E. Courtney, "Complex permittivity of GaAs and CdTe at microwave frequencies," *IEEE Trans. Microwave Theory Tech.*, vol. MTT-25, pp. 697-700, Aug. 1977.
- [5] M. W. Pospieszalski, "On the theory and application of the dielectric post resonator," *IEEE Trans. Microwave Theory Tech.*, vol. MTT-25, pp. 228-231, Mar. 1977.
- [6] J. K. Plourde and C. L. Ren, "Application of dielectric resonators in microwave components," *IEEE Trans. Microwave Theory Tech.*, vol. MTT-29, pp. 754-770, Aug. 1981.
- [7] H. E. Bussey, "Standards and measurements of microwave surface, impedance, skin depth, conductivity and Q ," *IRE Trans. Instrumentation*, vol. I-9, pp. 171-175, Sept. 1960.
- [8] F. J. Tischer and Y. H. Choung, "Anomalous temperature dependence of the surface resistance of copper at 10 GHz," *Proc. Inst. Elec. Eng. Microwaves, Opt. and Antennas*, vol. 129, part H, no. 2, pp. 56-60, Apr. 1982.
- [9] Y. Kobayashi and S. Tanaka, "Resonant modes of a dielectric rod resonator short-circuited at both ends by parallel conducting plates," *IEEE Trans. Microwave Theory Tech.*, vol. MTT-28, pp. 1077-1085, Oct. 1980.
- [10] Y. Kobayashi and S. Tanaka, "Discussions on dielectric rod resonator method of measuring complex dielectric constants," *Trans. IECE Japan*, vol. 59-B, pp. 223-230, Apr. 1976.
- [11] E. L. Ginzton, *Microwave Measurements*. New York: McGraw-Hill, 1957, pp. 403-405.
- [12] Y. Kobayashi, N. Fukuoka, and S. Yoshida, "Resonant modes for a shielded dielectric rod resonator," *Trans. IECE Japan*, vol. 64-B, pp. 433-440, May 1981. (Translated into English: *Electronics and Communications in Japan*, vol. 64-B, no. 11, pp. 44-51, Nov. 1981.)

*



Yoshio Kobayashi (M'74) was born in Gumma, Japan, on July 4, 1939. He received the B.E., M.E., and D. Eng. degrees in electrical engineering from Tokyo Metropolitan University, Tokyo, Japan, in 1963, 1965, and 1982, respectively.

He was a Research Assistant from 1965 to 1968, and a Lecturer from 1968 to 1982 in the Department of Electrical Engineering, Saitama University, Urawa, Saitama, Japan. He is now an Associate Professor at the same university. His current research interests are in dielectric waveguides and resonators, dielectric resonator filters, and measurement of dielectric materials in the microwave region.

Dr. Kobayashi is a member of the Institute of Electronics and Communication Engineers of Japan, and the Institute of Electrical Engineers of Japan.

*



Masayuki Katoh was born in Niigata, Japan, on April 8, 1954. He graduated from the Electrical Course at Ohmiya Technical High School, Ohmiya, Saitama, Japan, in 1973, and received in B.S. degree in electrical engineering from the Evening Division of Chuo University, Tokyo, Japan, in 1978.

Since 1973, he has been on the Faculty of Engineering at Saitama University, Urawa, Saitama, Japan, where he is a Technical Official. He is working on the measurement of dielectric materials in the microwave region.

Mr. Katoh is a member of the Institute of Electronics and Communication Engineers of Japan.